Microelectronic Engineering 87 (2010) 2582–2591

Contents lists available at ScienceDirect

Microelectronic Engineering

journal homepage: www.elsevier.com/locate/mee

Electrodynamically actuated on-chip flow cytometry with low shear stress for electro-osmosis based sorting using low conductive medium

Srinivasu Valagerahally Puttaswamy [a], Shilpa Sivashankar [a], Chia-He Yeh [b], Rong-Jhe Chen [a], Cheng Hsien Liu [a,b,*]

[a] Department of Power Mechanical Engineering, National Tsing Hua University, Taiwan
[b] Institute of NanoEngineering and Microsystems, National Tsing Hua University, Taiwan

ARTICLE INFO

Article history:
Received 26 March 2010
Received in revised form 18 June 2010
Accepted 14 July 2010
Available online 29 July 2010

Keywords:
Flow cytometry
Electro-osmosis
Dielectrophoresis
Cell sorting
Stem cells

ABSTRACT

In the proposed paper, we demonstrate on-chip electrodynamically driven actuator flow cytometry, based on negative dielectrophoretic (nDEP) focus and alternating current electro-osmotic flow (ACEOF) sorting technique. This single chip can perform three different functions such as focusing, transportation of beads/cells to detection site and reloading the unsorted ones with two distinctive phenomena. AC EOF is achieved by the design of the asymmetric electrode pair's array and nDEP is used to focus the beads/cells in-line. The design, simulation and experimental results of the proposed microchip are reported in this paper. The simulation and experimental results reveal well defined stable region for nDEP and ACEOF driving force. The potential severe shear stress damage caused by the sheath flow in conventional flow cytometry is eliminated. In addition, to explore the influence of conductivity of the medium, we have used low conductive formulated medium with conductivity of 81.4 μS/cm. The voltage and the frequency required to manipulate the particles decreased comparatively with the use of this medium.

1. Introduction

Flow cytometry is a powerful technique for the analysis of multiple parameters of individual cells within heterogeneous populations. The analysis is performed by passing thousands of cells per second through a laser beam and capturing the light that emerge from each cell as it passes through. The information regarding the size, type and content of cells can be derived through analysis of scattered light arising from individual cells. Flow cytometry has been used in applications such as immunology [1,2], cancer biology [3,4]. However, for environmental and clinical applications microflow cytometry is the preferred diagnostic tool [5–10]. Many flow cytometers have been fabricated using microsystem technologies among which, some use sheath flows while; others use sheathless flow for focusing [11].

Dielectrophoresis (DEP) is the movement of cells in non-uniform electric field. When the particle is more polarisable than the immersion medium, the resulting force will direct particles towards regions of electric field maxima at electrode edges. This phenomenon is known as positive dielectrophoresis (pDEP). The nDEP occurs when the cell is less polarizable than the suspending medium in a non-uniform electric field, and describes the movement of particles away from high field regions. Under, nDEP the particles are repelled by the electrodes and restricted to an area of low electric field between them. DEP finds a wide range of applications [12] such as, separation and isolation of cells [13,14], cell handling prior to electro fusion [15] or cell sorting [16]. The side effect of DEP is the temperature increase in the high conductivity medium in which the cells are suspended to disturb a favorable cellular environment [17]. The high conductivity medium requires high electric-fields environment to manipulate the beads/cells which might lead to a variety of profound biochemical and biophysical effects, such as apoptosis and cell-lyses [18].

EOF is the motion of liquid, induced by an applied potential across a capillary tube or microchannel. The cause of EOF is an electrical double layer (EDL) that forms at the stationary/solution interface. An electrical potential gradient arises in the vicinity of the solid–liquid interface due to the presence of net charge density. The region containing this electrical potential gradient is called EDL. When an external electrical field is applied to the liquid along the microchannel, the excess cations in the diffuse layer (mobile part) of the EDL will move towards the cathode. Because of the viscous force, these moving cations will drag the surrounding liquid to move with them and thus, result in the motion of a bulk movement. Because thickness of EDL compared with the channel dimension is very thin, the velocity profile of liquid flow is plug-like in the fully developed region. This is so-called EOF in which mean velocity is independent of the cross-sectional area of the channel.

* Corresponding author at: Microsystems and Control Laboratory, Department of Power Mechanical Engineering, National Tsing Hua University, Hsinchu 300, Taiwan. Tel.: +886 3 5715131x33706.
E-mail address: liuch@pme.nthu.edu.tw (C.H. Liu).

0167-9317/$ - see front matter © 2010 Elsevier B.V. All rights reserved.
doi:10.1016/j.mee.2010.07.023

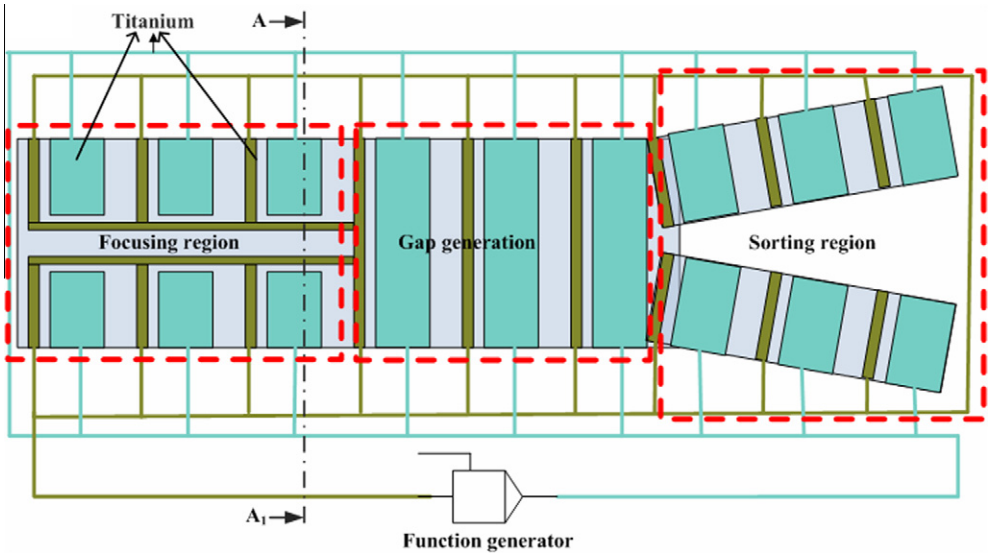

Fig. 1. Schematic diagram of the microchip representing the three regions performing three different functions.

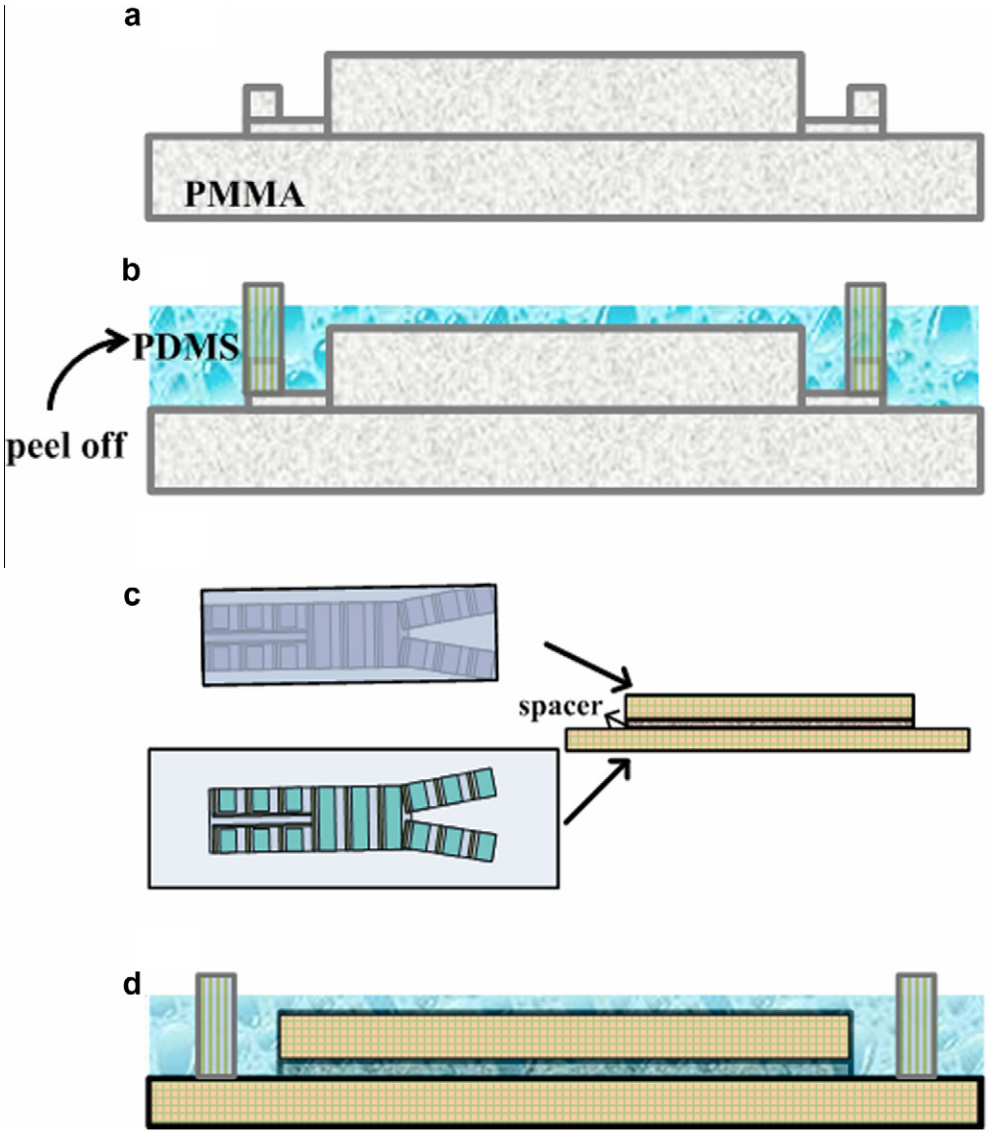

Fig. 2. Fabrication process of the device. (a) Engraved PMMA master mold. (b) PDMS poured on PMMA master mold. (c)The two identical glass substrates are placed one above the other with a PDMS spacer to enhance EOF and nDEP phenomena. (d) PDMS layer permanently bonded with the glass substrate after O_2 plasma treatment.

For chemical analysis, biological analysis and medical diagnosis transport and control of liquid samples at nanoscale is importunate. Hence EOF comes in handy for the microfluidic devices which have been utilized as the driving force to manipulate liquid samples [19]. EOF can occur in natural unfiltered water, as well as buffered solutions. EOF is used in wide range of applications such as chemical separation techniques, notably capillary electrophoresis [20], open channel electro-chromatography [21], preparative gel electrophoresis [22], the manipulation and separation of cells [23], and electro-spraying [24].

Numerous studies have reported the use of conventional hydrodynamic focusing with a large velocity ratio (sample flow: sheath flow), varying from 1:4 to 1:70 or even higher resulting in high shear stress [25]. In addition, conventional devices require bench top syringe pumps, controlled devices and complicated optical alignment procedure which result in bulk system and causes it to become expensive [26]. Electrokinetic (EOF and electrophoretic) focusing has been used previously to drive the fluid. However, the voltage of 150 and 2000 V were applied to the sample and waste reservoirs, respectively, which is of very high magnitude and is undesirable for a biological sample [27].

To overcome the above limitations, we have proposed electrodynamically actuated on-chip flow cytometry using nDEP for focusing beads/ cells with an ACEOF based sheathless flow, which results in elimination of the potential shear stress damage to sorted beads/cells. It requires lower sample volumes and reduces the amount of expensive reagents required for analysis. In addition we have used a low conductive medium that executes nDEP and ACEOF phenomenon with low frequency and voltage.

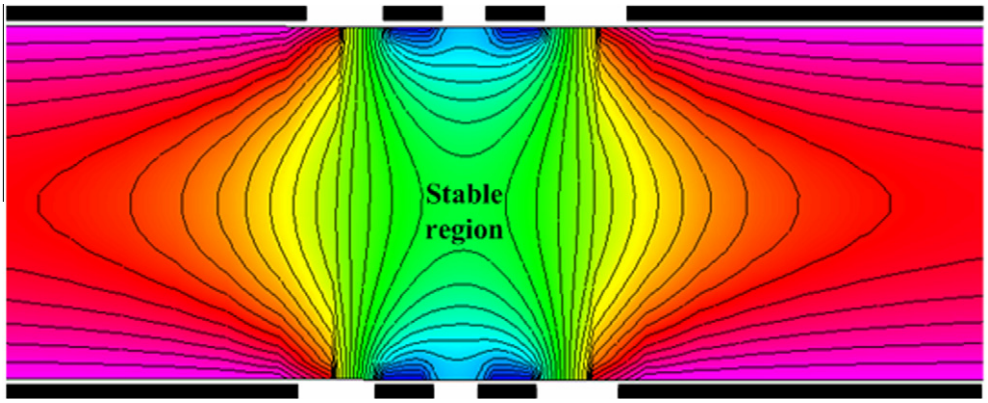

Fig. 3. CFD-ACE + simulation result indicating well defined stable region during nDEP phenomena at the Section A–A_1 shown in Fig. 1 for cell focusing.

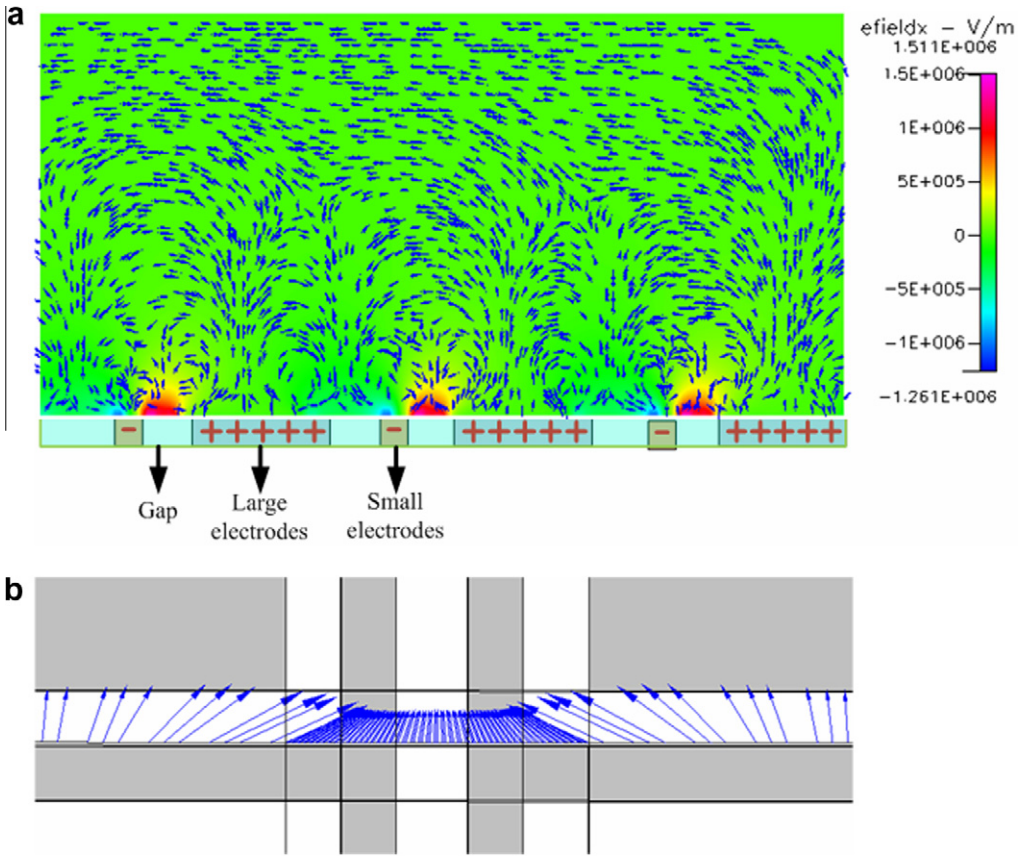

Fig. 4. CFD-ACE + simulation result elucidating EOF effect.(a) ACEOF net flow which drags beads/cells forward indicated by arrows (b) ACEOF plug flow around beads/cells while they move forward at the Section A–A_1 represented in Fig. 1.The arrows indicate the fluid flow direction and the grey region represent electrodes.

2. Experimental procedurals

2.1. Materials

Calcium chloride (anhyd), ferric nitrate, potassium chlorate, magnesium sulphate (anhyd), sodium chloride, sodium bicarbonate, sodium hypophosphate, D-glucose, sodium pyruvate, vitamins and amino acids were purchased from Sigma–Aldrich. Altered medium (pH 7.2) was used for all the experiments. All regents were of analytical grade and ultrapure water (resistance 18.36 MOhm/cm) produced by Millipore Milli-Q system was used throughout.

The latex particles used were polystyrene monodisperse microspheres (Polysciences, Warrington, PA, USA) with diameter of 8 μm and 15 μm. Before use, the beads were suspended at low concentration in formulated medium.

2.2. Design and fabrication of microchip

The glass substrate having asymmetric electrode array to provide ACEOF based electrodynamic effect is as represented in Fig. 1. The electrodes are well connected to obtain the desired effect.

To fabricate PDMS microfluidic chamber, we have used the master mold made of Poly methyl methacrylate (PMMA). The reason for using PMMA mold is the height of the microfluidic chamber being 1100 μm. The PMMA master mold is engraved by using engraving machine (Roland EGX-400) as represented in Fig. 2(a).

PDMS prepolymer is mixed with curing reagent with a 10:1 mass ratio and degassed in a vacuum chamber to remove the air bubbles. Silicon tubes are placed accurately at the inlet and outlet position on the PMMA master mold and PDMS is poured carefully. After degassing in a vacuum chamber again, PDMS is cured by heating-up in an oven. The PDMS layer is peeled off from the master mold as represented in Fig. 2(b). The two identical glass substrates with titanium electrode pattern are aligned and bonded together with PDMS spacer of 100 μm thick between them to enhance EOF and to prevent adhesion of beads/cells as represented in Fig. 2(c). To form a complete microfluidic device, the peeled PDMS layer is permanently bonded to the glass by applying O_2 plasma in O_2 plasma equipment as illustrated in Fig. 2(d). This plasma treatment also makes the walls of the microchannels hydrophilic, which is favorable to introduce the sample into the device. The complete device is connected to the external fluidic system via silicone tubes.

PDMS that is fabricated using PMMA master mold consists of two parts (i) the microfluidic channel and (ii) the microfluidic enclosing chamber. The width and the height of microfluidic channel are 500 μm and 100 μm, respectively. On the other hand, the width and the height of the microfluidic chamber are 5000 μm and 1100 μm, respectively.

A commercial finite element software CFD-ACE+ (CFDRC, Huntsville, AL) was used to simulate the electric field. The CFD-ACE+ simulation software has wide range of application and has been used by our group to simulate electric field distribution and microfluidic flow pattern [28–31]. While simulating for nDEP and ACEOF phenomena the following boundary conditions are set: (a)

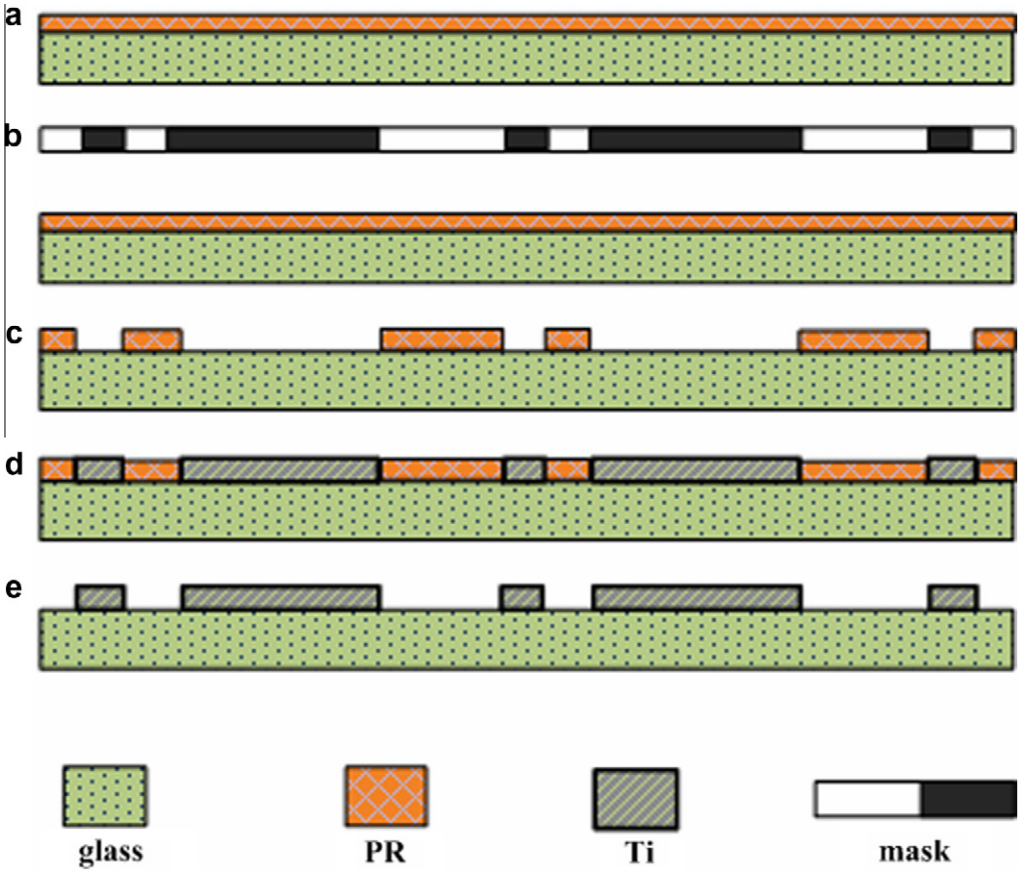

Fig. 5. Microfabrication process for titanium electrodes on glass substrate. (a) Photoresist (PR) was spun coated on a glass substrate. (b) Photoresist was exposed to UV rays through a mask. (c) Patterned photoresist structures after developing. (d) Titanium deposited by E-Gun Evaporation. (e) Fine patterned titanium electrodes obtained by lift-off process.

Table 1
Composition of the modified medium used for DEP manipulation along with native culture medium.

Components	DMEM (mg/l)	DEP buffer (mg/l)	Altered medium (mg/l)
HEPES	–	2385	
Sucrose	–	80.7 (g/l)	95 (g/l)
Dextrose	4500	10.6 (g/l)	2250
Amino acids	100% as per catalog	–	15% of DMEM
Vitamins	100% as per catalog	–	15% of DMEM
Salts			
$CaCl_2$	200	11.1	20
$Fe(NO_3)_3{\cdot}9H_2O$	0.1	–	0.001
KCl	400		4
$MgSO_4$ (anhyd)	97.67		0.98
NaCl	6400		64
NaH_2PO_4	125		1.25
Sodium pyruvate	110		1.1

More detailed information about composition of DMEM (12,800) can be found in INVITROGEN cell culture catalog 2008/2009.

the boundary conditions on the channel walls are set to zero flow velocity based on a non slipping assumptions. (b) The nDEP and ACEOF force is applied via ac potentials of 8 Vpeak–peak on the individual sorting electrode with ac frequency of 1000 Hz and 500 Hz, respectively. (c) The boundary conditions at the inlet and outlet are set up as fixed pressure. (d) For electro-osmosis the zeta potential is constant with a value of 0.04 V. Debye's thickness is set as constant with a value of 3×10^{-9} m.

The CFD-ACE+ simulation results divulge the stable region in the focusing area as represented in Fig. 3. The simulation of ACEOF effect, which drags beads/cells forward due to the net flow is indicated by arrows in the Fig. 4(a). The plug flow which keeps beads/cells in-line while they move forward is elucidated in Fig. 4(b).

A chip with titanium electrodes were designed and fabricated on a glass substrate using photolithography process, which has been widely used for making the microchips. In this technique; electrodes were generated using light, light-sensitive photoresist AZ5214 and chrome on glass mask. At first, the photoresist was spun coat on a clean glass substrate and exposed to ultraviolet (UV) light through a customized mask containing the desired opaque pattern aligned by EV620 mask aligner. The exposed part of the photoresist was solubilized in a developer solution, resulting in a photoresist pattern. Electrodes were micromachined on a glass substrate by the photolithography process with the E-Gun evaporation of a 200 Å titanium layer. Finally, the fine titanium electrodes were obtained via the lift-off process as illustrated in Fig. 5.

2.3. Preparation of medium

Medium with optimal conductivity, osmolarity and pH was prepared mainly by varying the salt concentration. The native culture medium Dulbecco's Modified Eagle Media (DMEM) has high conductivity (18.56 mS/cm) due to high salt concentration hence, was not used for manipulation. The frequency and voltage required for DMEM is very high and this decreases the viability of cells [32]. Hence a medium composing of sucrose and dextrose with fairly increased 10% of calcium chloride with 1% of DMEM salt concentration was used for manipulation of beads/cells. The medium has all the components of native culture medium with the reduced quantity. This medium can be conveniently used to demonstrate nDEP and ACEOF phenomena for Hep G2, Human Mammary Epithelial Cell (HMEC), Human Endothelial Kidney293 (HEK) and latex beads. The compositions of the media are presented in Table 1.

2.4. Measurement of conductivity, osmolarity and pH of the media

Conductometer (WTW cond 330i Germany) was used to determine the conductivity of the media. The instrument is calibrated by using a standard which is as close as possible to the solution being measured (1413 μS/cm). The probe used to measure conductivity was originally an amperometric system. Probes with different electrode spacing allow measurement of various conductivities. This method applies a known potential (voltage, V) to a pair of electrodes and measures the current (I). An alternating voltage applied to one of the electrodes causes the ions in the solution to migrate towards the other electrode. The more the ions in the solution, the greater will be the current. At first, the instrument measures the current and uses Ohm's law to calculate the conductance of

Table 2
Measured values of pH, conductivity, and osmolarity of media.

Parameters at 25 °C	DMEM	DEP buffer	Altered medium
pH	7.2	6.8	7.1
Conductivity (μS/cm)	18,560	102	81.4
Osmolarity (mOsm/kg)	320	360	330

All the values of the medium are well within the physiological values.

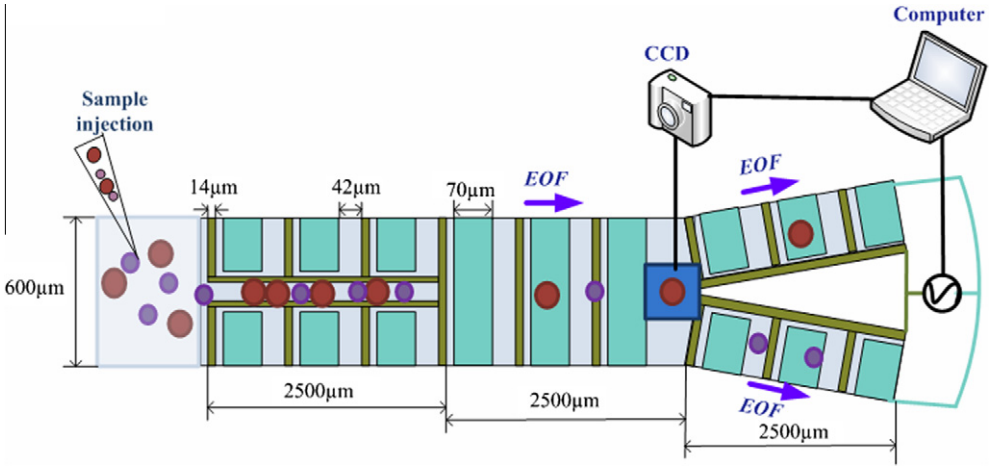

Fig. 6. Schematic view of the experimental setup illustrating the working principle of the sorting microchip. CCD connected to the Lab View programming provides image recognition feedback for beads/cells sorting.

the solution and then by taking the cell data into account the conductivity of the solution is determined. To minimize the influence of temperature during the process of conductivity measurement, all the readings were recorded at 25 °C. If the temperature of the solution is more than 25 °C, it is allowed to cool down and then the conductivity is measured.

Osmolarity was measured using Advanced Instruments Micro Osmometer 3300 (Norwood, Massachusetts, USA). The pH was measured using Eutech Instruments pH 1500. All readings were recorded at a temperature of 25 °C. The average value of all the readings was determined from at least three measurements.

2.5. Experimental set up for DEP based cell sorting

To generate the out-of-phase ac voltage for DEP and ACEOF operation on the microchip, a function generator (33120A, Agilent) was employed. An oscilloscope (54624A, Agilent, USA) was used to check the input electrical signals. An inverted microscope (BX51, Olympus, Tokyo, Japan) was put forth to keep track of the motions and displacements of the cells. Movies and images were captured and recorded via a digital CCD-camera connected to a computer.

Fig. 6 illustrates the working principle of an electrodynamically driven actuator on-chip flow cytometry. The beads/cells in the for-

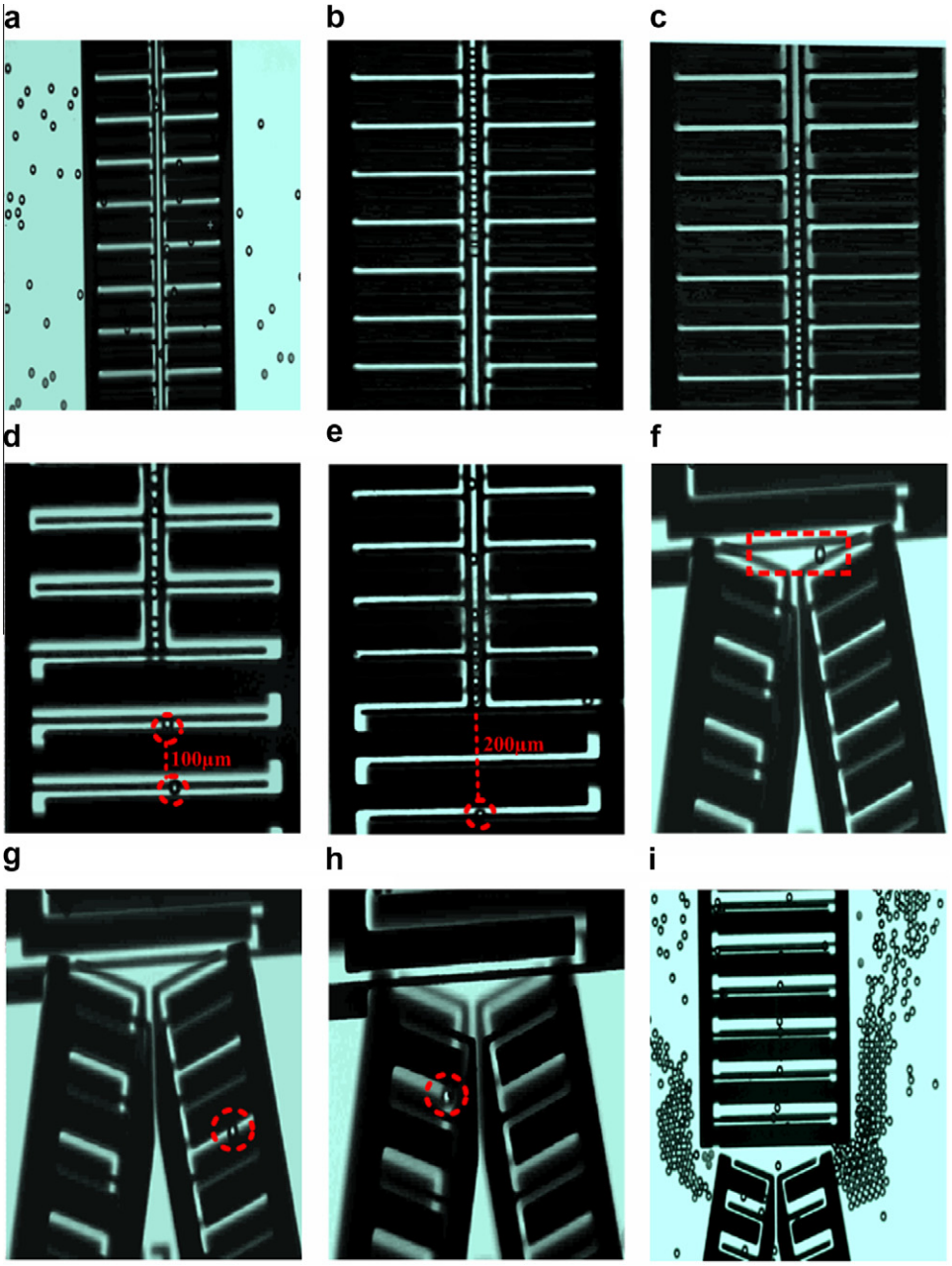

Fig. 7. On chip manifestation of beads/cells sorting. (a) Random distribution – the beads/cells injected will exhibit random distribution after loading onto microchip. (b) Line-up – the beads are focused to line-up in between electrodes due to nDEP phenomena. (c) March – the beads/cells so lined-up will move forward due to ACEOF phenomena in the absence of sheath flow. (d and e) Gap generation – the gap will be generated between the beads/cells depending on the size. (f) Detection – the beads/cells approaching this defined region will be detected by CCD, programmed by Lab View image recognition software. (g and h) Sorting – Lab View image recognition system recognizes the beads/cells of the same size or property and deflects them to right or left arm of electrodes accordingly. The beads of 8 μm are deflected to the right arm and beads of 15 μm are deflected to the left arm. (i) Reloading – the unsorted beads/cells around the chip are reloaded to the system for further sorting.

mulated medium are introduced to the focusing region where in, they are focused to line-up due to nDEP force. When applied with suitable voltage and frequency the beads/cells are dragged forward by ACEOF force. There will be a gap generation between individual adjacent lined-up cells when they enter second stage. Finally beads/cells are sorted individually by using CCD with Lab View image recognition system and the unsorted ones are reloaded into the microchip for further sorting.

3. Results and discussion

3.1. Conductivity, osmolarity and pH of the media used

Table 2 elucidates the measured values of all the parameters mentioned above. The conductivity of the medium was reduced and is well suited for DEP manipulation. The osmolarity values are well within the physiological values obtained for DMEM from the literature (300–340 mOsm/kg) [33].The measured pH value of the medium was also well within the physiological values (7–7.4).

3.2. Sorting manifestation

Fig. 7(a–i) demonstrates the sorting feature of the chip. Fig. 7(a) depicts the random distribution of beads/cells loaded on the chip. The frequency and voltage is varied after the introduction of beads/cells into the focusing region. At a voltage of 2 Vpeak–peak and a frequency of 800 Hz, nDEP phenomena can be clearly observed and hence the randomly distributed beads/cells are moved towards the stable region of minimum electric field, focused to line-up locally in the main flow path as shown in Fig. 7(b). The

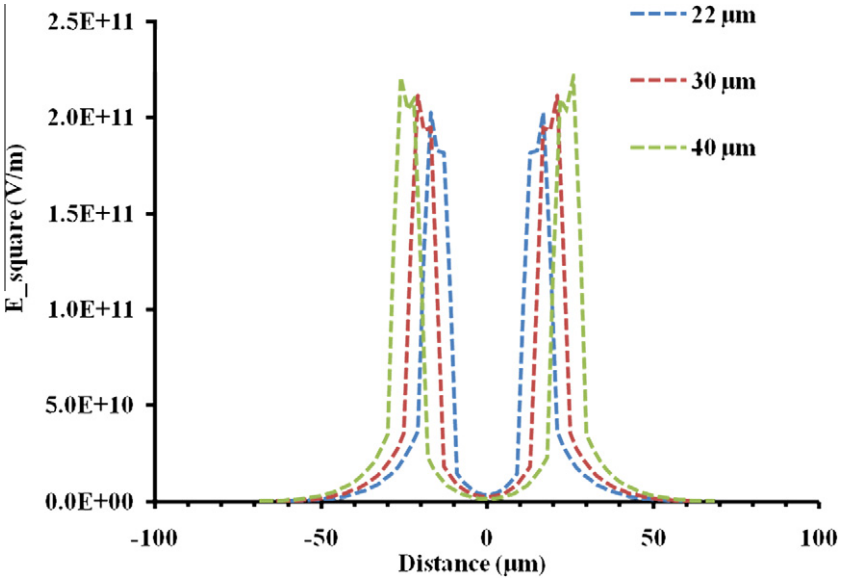

Fig. 8. Width of the stable region between electrodes for varying distance between a pair of electrodes. This is an important criterion during nDEP for alignment of the beads/cells in the stable region.

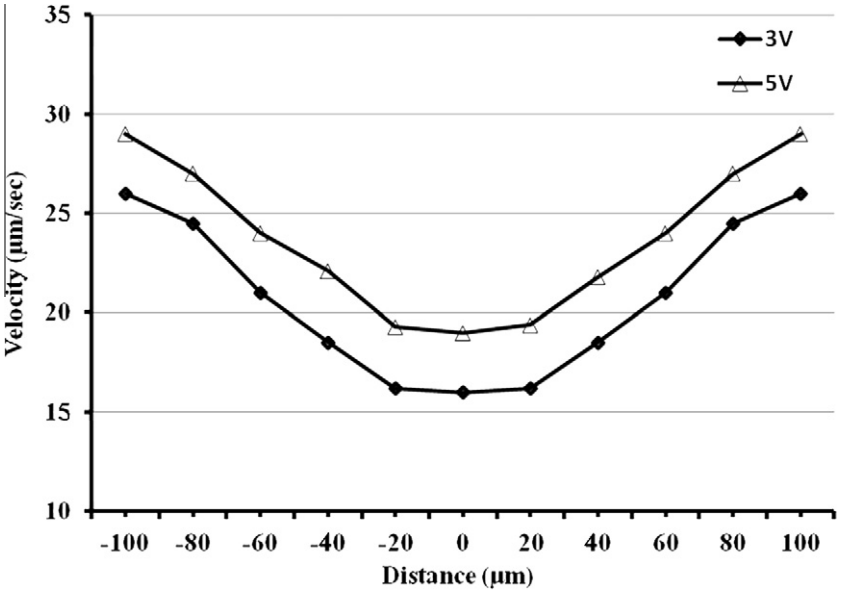

Fig. 9. Flow velocity distribution at the Section A–A_1 along the focusing region as represented in Fig. 1. The flow velocity around the lined-up beads/cells is almost uniform due to plug flow, indicating the absence of shear stress.

stable region is indicated by CFD-ACE+ simulation result in Fig. 3. From the demonstration of the nDEP phenomenon it is evident that, the required focus length is obtained without any shear force acting on the cell due to the sheathless and the plug flow. The absence of a sheath means no dilution, which allows small amount of sample and less waste. Focus length is defined as the length to reach a focused stream and large velocity ratio is required to achieve shorter focus length in the earlier reported flow cytometry [25].

Another most important aspect of flow cytometry is to ensure the single-file passing of the cells. In conventional flow cytometry, this can be achieved by focusing the cell solution to the center of the flow tube with the sheath flow using a co-axial injection flow chamber, which results in high shear stress on the bio-sample. Hence, in the proposed device the width of the stream can be focused and accurately controlled by simulating the distance between the electrodes such that individual cells pass sequentially through the detection region for sorting purpose. The above mentioned fact is also supported by Fig. 8. If the distance between the electrodes is 22 μm, 30 μm and 40 μm the width of the stable region will be 18 μm, 26 μm and 36 μm, respectively.

Furthermore variations in voltage and frequency results in ACEOF. When the required AC potential is applied to these asymmetric electrodes, a uni-directional flow can be generated by the gradient of the electric field. Breaking symmetry in the widths and spacing of each electrode pair in the array produces a nonsymmetrical local flow that eventually generates a global flow in the direction of broken symmetry [34]. Rolling motion of the fluid is generated at every electrode edge, the magnitude of the velocity depending on the tangential derivative of the electrical energy stored in the double layer at that location [35].Responding to the frequency of AC potential applied; the net ACEOF is induced resulting from both capacity charging and faradic charging effects. At a voltage of 3 Vpeak–peak and a frequency of 500 Hz, the lined-up beads/cells move forward by the drag forces induced by the ACEOF on electrode array as represented in Fig. 7(c) which is supported by the simulation result of ACEOF effect as elucidated in Fig. 4(a). The flow velocity around the lined-up beads/cells is illustrated in Fig. 9 from which it is evident that the flow is of plug flow type in which the velocity of the fluid is constant across any cross-section of the focusing region. The flow velocity is uniform for a length of 20 μm across the channel from the center of the channel for an applied voltage of 3 Vpeak–peak and 5 Vpeak–peak. When the beads/cells are focused by the nDEP force and carry forward by ACEOF, they will not experience shear force due to plug flow around them. Besides, the ACEOF driving effect also keeps the beads/cells in-line while, they move forward as indicated by the arrows in Fig. 4(b).

Fig. 7(d and e) demonstrates the generation of gap between adjacent lined-up beads/cells. As the distance between adjacent beads/cells are longer, when approaching the detection region as represented in Fig. 7(f) they are sorted individually by using CCD with Lab View image recognition system. The beads/cells from the detective region are deflected towards left or right arm based on their size as shown in Fig. 7(g and h), respectively. This detection arrangement permits the sorting of beads/cells without the need for an expensive microscope, or the requirement for delicate optical alignment system. In conventional 2D hydrodynamic focusing, lack of vertical focusing may result in two or more cells simultaneously entering the detection region, causing spreading of the cells and large measurement errors [36,37]. However, the proposed microchip is well designed to generate sufficient gap between two consecutive beads/cells before entering the detection region to overcome the above problem.

The throughput of the device is around 15 beads/cells per min which is less compared with the fastest of 30 cells per second taking advantage of electrokinetic drive, reported by Dittrich et al. [38]. Meanwhile some research indicates that some stem cells, such as MSC (Mesenchymal Stem Cell), are practically sensitive to the shear stress and other mechanical loading. Due to shear stress stimulation, MSC may either change into another cell or change its physiology which is undesirable [39]. Due to the absence of shear stress the proposed microchip can be conveniently used for stem cell sorting to overcome the above mentioned problem.

3.3. Influence of voltage and frequency

The low conductivity DEP buffer has been used for liver cell patterning to mimic liver lobule in our group [17]. However, the DEP buffer is excellent for DEP manipulation, but it is unsuitable as the

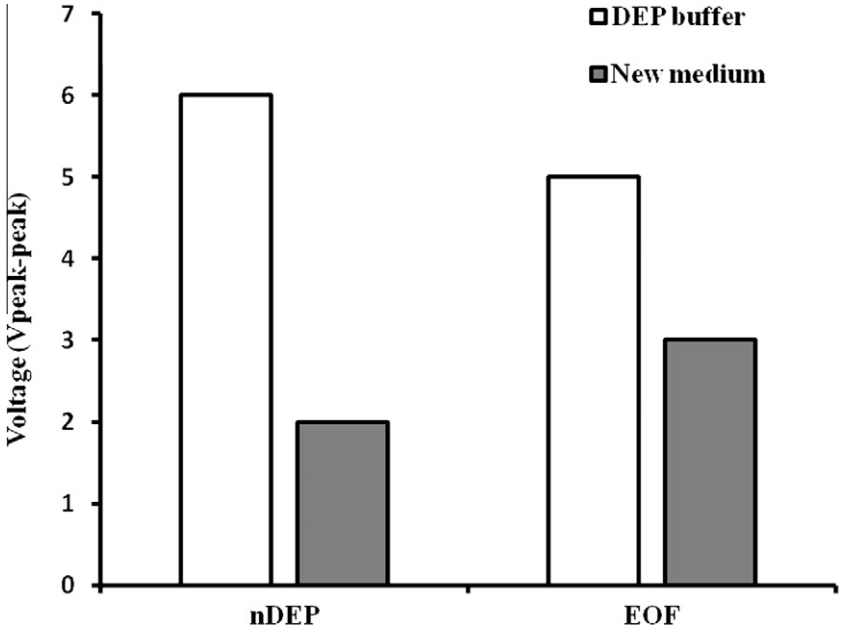

Fig. 10. Comparison of voltage required to demonstrate nDEP and ACEOF phenomena.

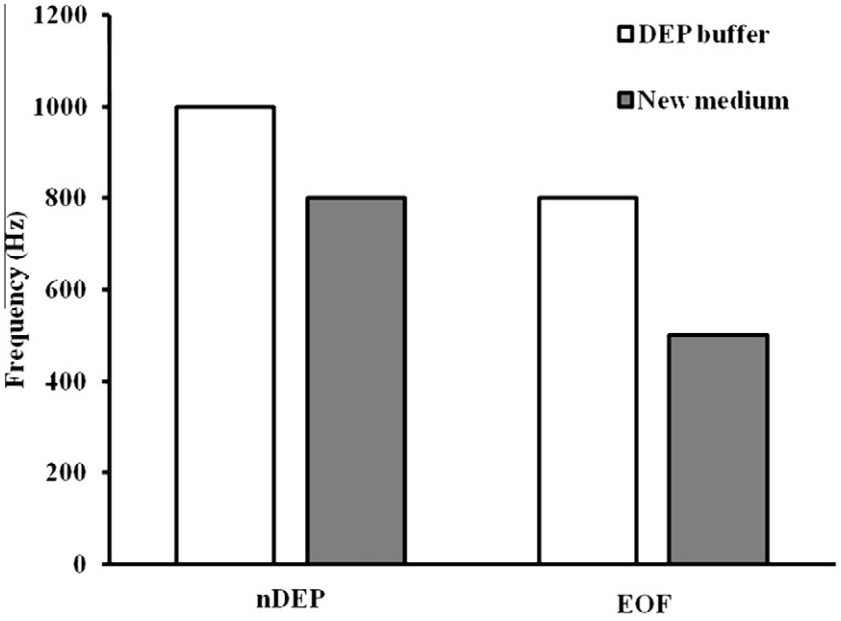

Fig. 11. Comparison of frequency required to demonstrate nDEP and ACEOF phenomena.

voltage and the frequency required are still high. Experiments were carried out with both DEP buffer and low conductive medium to measure the minimum voltage and frequency required to execute phenomena of nDEP and ACEOF. As represented in Figs. 10 and 11 nDEP phenomena can be clearly observed at 2 Vpeak–peak at 800 Hz and ACEOF phenomena can be visualized at 3 Vpeak–peak at 500 Hz in the new low conductivity medium. The voltage and the frequency required for both nDEP and ACEOF modes are less compared to the DEP buffer without any limitation to either the diminutive electrode size or the advanced fabrication technology. The low voltage also results in reduced Joule heating. This condition is favorable for bio-samples as increased Joule heating can result in low efficiency of column separation, reduction of analysis resolution, and even loss of introduced samples [40–47]. Joule heating may create temperature gradient and can also cause increase in temperature [48]. Finally the unsorted beads/cells are reloaded into the chip as represented in Fig. 7(i) and the sorting process is repeated.

4. Conclusions

In summary, we have successfully developed microchip flow cytometry using micromachining technology to demonstrate the sheath-free sorting phenomenon of beads/cells based on nDEP focusing and ACEOF induced flow. The use of low conductive medium favors the desired cellular environment. The voltage and the frequency required to manipulate beads/cells are considerably reduced with the use of this medium. The detection arrangement performs the sorting operation without the need of an expensive microscope and other delicate optical instruments. The proposed microflow cytometry is cost effective, portable, consumes less sample and functions without the need of heavy instrumentation.

Acknowledgements

This research was financially supported by National Science Council under grant NSC 98-2120-M-007-003. The authors thank Prof. Hsing-Wen Sung and Mr. Kiran Sonje for helping osmolarity measurements and helpful discussion. The formulated media were prepared with the help from Prof. Chin Yu and Dr. Sepuru Krishnamohan. Authors thank Prof. H.Y Chang for helpful discussion on DEP media and Mr. Tung-Ming Yu for helping us in Lab View set up. The authors thank the Semiconductor Research Center and National Nano Device Laboratory for the access of microfabrication facility.

References

[1] S.L. Liang, M. Slattery, D. Wagner, S.I. Simon, C. Dong, Ann. Biomed. Eng. 36 (2008) 661–671.
[2] S.L. Liang, C. Fu, D. Wagner, H. Guo, D. Zhan, C. Dong, M. Long, Am. J. Physiol. 294 (2008) C743–C753.
[3] J. You, A.M. Mastro, C. Dong, Exp. Cell Res. 248 (1999) 160–171.
[4] C. Dong, M.J. Slattery, B.M. Rank, J. You, Ann. Biomed. Eng. 30 (2002) 344–355.
[5] J. Porter, D. Deere, M. Hardman, C. Edwards, R. Pickup, FEMS Microbiol. Ecol. 24 (1997) 93–101.
[6] A. Agronskaia, J.M. Schins, B.G.D. Grooth, J. Greve, Anal. Chem. 71 (1999) 4684–4689.
[7] S. Gawad, L. Schild, P. Renaud, Lab Chip 1 (2001) 76–82.
[8] M. Rieseberg, C. Kasper, K.F. Reardon, T. Scheper, Appl. Microbiol. Biotechnol. 56 (2001) 350–360.
[9] J. Ho, Anal. Chim. Acta. 457 (2002) 125–148.
[10] J.W. Grate, C.J. Bruckner-Lea, A.E. Jarrell, D.P. Chandler, Anal. Chim. Acta. 478 (2003) 85–98.
[11] S.C. Hur, H.T. Kwong Tse, D.D. Carlo, Lab Chip 10 (2010) 274–280.
[12] M.P. Hughes, Nanoelectromechanics in Engineering and Biology, CRC Press LLC, Boca Raton, Florida, 2002.
[13] X.B. Wang, Y. Huang, J.P.H. Burt, J. Appl. Phys. 26 (1993) 1278–1285.
[14] G.H. Markx, Y. Huang, X.F. Zhou, Microbiology 140 (1994) 585–591.
[15] S. Masuda, M. Washizu, T. Nanba, IEEE Trans. Ind. Appl. 25 (1989) 732–737.
[16] M. Washizu, T. Nanba, S. Masuda, IEEE Trans. Ind. Appl. 26 (1990) 352–356.
[17] C.T. Ho, R.Z. Lin, W.Y. Chang, H.Y. Chang, C.H. Liu, Lab Chip 6 (2006) 724–734.
[18] U. Zimmermann, U. Friedrich, H. Mussauer, P. Gessner, K. Hamel, V. Sukhorukov, IEEE Trans. Plasma Sci. 28 (2000) 72–82.
[19] D.J. Harrison, K. Fluri, K. Seiler, Z. Fan, C.S. Effenhauser, A. Manz, Science 261 (1993) 895–897.
[20] D.J. Harrison, A. Manz, Z. Fan, H. Lüdi, H.M. Widmer, Anal. Chem. 64 (1992) 1926–1932.
[21] S.C. Jacobson, R. Hergenröder, L.B. Koutny, J.M. Ramsey, Anal. Chem. 66 (1994) 2369–2373.
[22] M. Hayakawa, Y. Hosogi, H. Takiguchi, T. Shiroza, Y. Shi-bata, K. Hiratsuka, M.K. Kishikawa, S. Hamajima, Y. Abiko, Anal. Biochem. 313 (2003) 60–67.
[23] P.C.H. Li, D.J. Harrison, Anal. Chem. 69 (1997) 1564–1568.
[24] R.S. Ramsey, J.M. Ramsey, Anal. Chem. 69 (1997) 1174–1178.
[25] G.B. Lee, C.I. Hung, B.J. Ke, G.R. Huang, B.H. Hwei, ASME J. Fluids Engg. 123 (3) (2009) 672–679.
[26] L.M. Fu, R.J. Yang, C.H. Sin Lin, Anal. Chem. Acta. 507 (2004) 163–169.
[27] A.M. Maxine, T.C. Christopher, C.J. Stephen, J.R. Michael, Anal. Chem. 73 (2001) 5334–5338.
[28] T.C. Shih, K.H. Chu, C.H. Liu, J Microelectromech. Syst. 16 (2007) 816–825.

[29] C.T. Kuo, C.H. Liu, Lab Chip 8 (2008) 725–733.
[30] H.Y. Wu, C.H. Liu, Sens. Actuators A 118 (2005) 107–115.
[31] C.T. Ho, R.Z. Lin, H.Y. Chang, C.H. Liu, Lab Chip 5 (2005) 1248–1258.
[32] S.T. Rupert, M. Hywel, G.G. Nicolas, Lab Chip 9 (2009) 1534–1540.
[33] A. Bouaziz, A. Richert, A. Caprini, Biomaterials 17 (1996) 2281–2287.
[34] A.B.D. Brown, C.G. Smith, A.R. Rennie, Phys. 63 (2001) 1–8.
[35] A. Ajdari, Phys. 61 (2000) R45–R48.
[36] A. Wolff, I.R. Perch-Nielsen, U.D. Larsen, P. Friis, G. Goranovic, C.R. Poulsen, J.P. Kutter, P. Telleman, Lab Chip 3 (2003) 22–27.
[37] S. Chung, S.J. Park, J.K. Kim, C. Chung, D.C. Han, J.K. Chang, Microsyst. Technol. 9 (2003) 525–533.
[38] P.S. Dittrich, P. Schwille, Anal. Chem. 75 (2003) 5767–5774.
[39] C.E. Jr George, L.S. Virna, E.M. Jr John, S.S. Michael, Biomaterials 27 (2006) 6083–6095.
[40] J.H. Knox, K.A. McCormack, Chromatographia 38 (1994) 207–214.
[41] J.H. Knox, K.A. McCormack, Chromatographia 38 (1994) 215–221.
[42] E. Grushka, R.M. McCormick, J.J. Kirkland, Anal. Chem. 61 (1989) 241–246.
[43] A.E. Jones, E. Grushka, J. Chromatogr. 466 (1989) 219–225.
[44] M.A. Bosse, P. Arce, Electrophoresis 21 (2000) 1018–1025.
[45] M.A. Bosse, P. Arce, Electrophoresis 21 (2000) 1026–1033.
[46] K. Swinney, D.J. Bornhop, Electrophoresis 23 (2002) 613–620.
[47] W.A. Gobie, C.F. Ivory, J. Chromatogr. 516 (1990) 191–210.
[48] G.Y. Tang, C. Yang, J.C. Chai, H.Q. Gong, Int. J. Heat Mass Trans. 47 (2004) 215–227.